



Evaluation of extensive floods in western/central Europe

Blanka Gvoždíková¹ and Miloslav Müller^{1,2}

¹Faculty of Science, Charles University, Prague, Czech Republic

²Institute of Atmospheric Physics AS CR, Prague, Czech Republic

Correspondence to: Blanka Gvoždíková (gvozdikb@natur.cuni.cz)

Received: 22 September 2016 – Discussion started: 27 October 2016

Revised: 23 April 2017 – Accepted: 6 June 2017 – Published: 21 July 2017

Abstract. This paper addresses the identification and evaluation of extreme flood events in the transitional area between western and central Europe in the period 1951–2013. Floods are evaluated in terms of three variants on an extremity index that combines discharge values with the spatial extent of flooding. The indices differ in the threshold of the considered maximum discharges; the flood extent is expressed by a length of affected river network. This study demonstrates that using the index with a higher flood discharge limit changes the floods' rankings significantly. It also highlights the high severity events.

In general, we detected an increase in the proportion of warm half-year floods when using a higher discharge limit. Nevertheless, cold half-year floods still predominate in the lists because they generally affect large areas. This study demonstrates the increasing representation of warm half-year floods from the northwest to the southeast.

1 Introduction

Hydrological events, especially floods, are serious natural hazards in western and central Europe (Kundzewicz et al., 2005; Munich Re, 2015). Several extreme floods occurred in western and central Europe, e.g., in August 2002, January 2003, March/April 2006, and June 2013. The last was one of the largest in some river basins over the last 2 centuries (Blöschl et al., 2013).

In addition to river floods, flash floods affect this part of Europe, although these are mostly local events that usually produce less damage (Barredo, 2007). Therefore, we are interested in extensive floods affecting several river basins. Uhlemann et al. (2010) call these floods trans-basin. They are usually triggered by persistent heavy rainfall and/or

snowmelt. Differences in the causes of river floods can be detected between the western and central parts of Europe. Western Europe experiences flooding primarily during the cold half of the year due to zonal westerly circulation systems (Caspary, 1995; Jacobeit et al., 2003). Towards the east, warm half-year floods become more frequent. This is largely due to cyclones moving along the Vb pathway described by van Bebber (1891). These cyclones move from the Adriatic in a northeasterly direction (e.g., Nissen et al., 2014), and the “overturning” moisture flux brings warm and moist air into the central part of Europe (Müller and Kašpar, 2010). However, it is not possible to delineate the borders of western and central Europe precisely with respect to differences in their flood events because of a broad transitional zone where both types of flooding occur.

An extremity index is useful for comparing individual flood events and determining their overall extremity. Various indicators and indices are used for the assessment of extreme events (including floods) and in their quantitative comparison. Different approaches are applied because the definition of event extremity is not uniform (Beniston et al., 2007), so various sets of extreme floods have been compiled in individual papers. The assessment of extreme floods is based on the quantification of human and material losses (severity), high discharge values (intensity), peak discharge return periods (rarity), or a combination of these indicators. The ranking of the largest floods can differ depending on which aspect of extremity was evaluated.

An assessment based on flood severity may be a simple way to evaluate a flood's extremity. Barredo (2007) identified major flood events in the European Union between 1950 and 2005 to create a catalog and map of the events. He utilized two simple selection criteria: damage amounting to at least

0.005 % of EU GDP and a number of casualties higher than 70.

Other authors prefer evaluations based on the intensity or rarity of flooding because these aspects better reflect causal natural processes. Some authors classified floods into extremity classes based on the observed water levels (Brázdil et al., 1999; Mudelsee et al., 2003), which is most suitable for long-term pre-instrumental flood records. Water level values for individual flood events are at our disposal due to high water marks, chronicle records or other documents. This type of flood extremity evaluation was applied to the long-term flood records of the Basel gauge station on the Rhine River (Brázdil et al., 1999) and in the Elbe and Oder River basins (Mudelsee et al., 2003).

Additionally, Rodda (2005) used maximum discharges to express flood extremity in the Czech Republic. He considered the ratio of the maximum mean daily discharge to the median annual flood. This was completed for each station and flood event to study the spatial correlations among flood intensities in various basins.

Rarity can be used to compare extreme floods at different locations, when extremity is defined not by absolute thresholds (e.g., discharge values), but by relative ones (e.g., n th quintile of the dataset). Keef et al. (2009) focused on the spatial dependence of extreme rainfall and discharges in the UK and used return periods to define extreme values. Their work confirms that it is possible to compare the event extremities at different locations, even when the actual discharge values vary considerably.

Comprehensive indicators of flood extremity typically combine some aspect of extremity or consider other factors, such as the areal extent or duration of events. When creating these indicators, researchers attempt to add information about flooding from all locations where it was observed. The Francou index k (Francou and Rodier, 1967; Rodier and Roche, 1984; Herschy, 2003) is one of the older indices that assess flood extremity only at a particular station. In the Francou index, the common logarithm of maximum discharge is divided by the common logarithm of the catchment area (Rodier and Roche, 1984; Herschy, 2003). Among others, it was used to evaluate the largest floods in the World Catalogue of Maximum Observed Floods (Herschy, 2003).

Müller et al. (2015) designed a more complicated extremity index using return periods of peak discharges. They present 50 maximum floods in the Czech Republic for the period 1961–2010, which are identified based on the so-called flood extremity index (FEI) (Müller et al., 2015). In addition to the peak discharge return periods, the size of the relevant basin is considered for each location. The authors also suggested extremity indices other than the FEI that are applicable to precipitation events: the weather extremity index (Müller and Kašpar, 2014) and the weather abnormality index. Comparison of these indices with the FEI may aid in examining the relationship between precipitation and flood extremity (Müller et al., 2015).

To analyze the spatial and temporal distribution of floods in Germany, Uhlemann et al. (2010) developed a comprehensive method for the identification and evaluation of major flooding affecting several river basins. They used a time series of mean daily discharges and searched for simultaneously occurring significant discharge peaks comprising individual flood events. Their index accounts for the spatial extent of flooding (expressed by the length of the affected rivers) and discharge peak values exceeding the 2-year return value. The authors present 80 major flood events in Germany from 1952 to 2002.

Subsequently, Schröter et al. (2015) adopted the approach of Uhlemann et al. (2010) and compared several major floods in Germany. Their modified index compiled only those maximum discharges that exceeded the 5-year return value; the discharges were normalized by the respective 5-year return values and weighted by the portion of the affected river length. The final index equals the sum of these values from affected stations. Thus, the indices by Uhlemann et al. (2010) and Schröter et al. (2015) differ only in the threshold of the discharge values entered into the index calculation (2- and 5-year return values, respectively). However, Schröter et al. (2015) presented only the June 2013 flood extremity in comparison with two other major floods in August 2002 and July 1954. Because other major flood events were not presented for comparison, it is not possible to precisely identify the influence of this methodological change on their results.

The main aim of this paper is to present lists of extreme flood events from the period 1951–2013 and describe their spatial and temporal distribution. The flood events are selected on the basis of extremity indices with different thresholds of the considered maximum discharges. The discussion of the role of discharge thresholds in the floods' rankings is a part of the paper. The presented indices are based primarily upon the approach of Uhlemann et al. (2010). Each of the indices combine the flood discharge magnitude with the spatial extent of flooding.

The area of interest might be called “Midwestern” Europe and is basically a transitional area between western and central Europe. It has natural boundaries: the Alps to the south, the Carpathian Mountains and Lesser Poland Upland to the east and the coasts of the North and Baltic seas to the north-west and the north. The area is defined by six main river basins: Rhine, Elbe, Oder, Weser, Ems, and Danube up to Bratislava. As mentioned above, this area is interesting because of a noticeable shift in the seasonality of floods in a west-to-east direction. Due to its heterogeneity and vastness, the area is also convenient for index design assessment when evaluating the extremity of floods affecting several river basins.

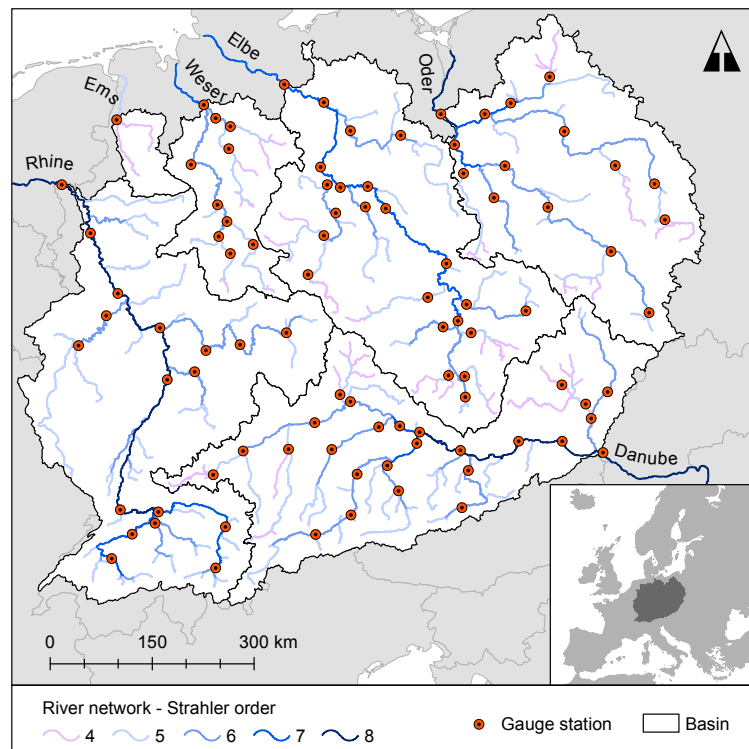


Figure 1. Gauge stations in the area of interest. Strahler stream order is distinguished by color.

2 Data and methods

2.1 Data

We used mean daily discharge values at selected stations (for each day during the period 1951–2013) as a basis when searching for floods that occurred simultaneously within the study area. Only data from stations enclosing at least 2500 km² of the relevant river basin were used due to poor data availability for smaller catchments and to exclude minor floods. This work is based primarily on data that were obtained from the database of the Global Runoff Data Centre (GRDC, 2017), an international archive of monthly and daily discharges. The time series was incomplete in some cases, so we used additional data from national hydrological yearbooks, the Czech Hydrometeorological Institute, the Austrian server eHYD (2016) and the Polish Institute of Meteorology and Water Management – National Research Institute (IMGW-PIB, 2017). When necessary, missing values were obtained using linear regression.

As a result, 93 gauging stations from seven countries (the Czech Republic, Slovakia, Poland, Austria, Switzerland, Germany and the Netherlands) were selected to analyze the time series of mean daily discharges between 1951 and 2013. The study area is approximately 579 000 km², with the length of the river network reaching almost 17 700 km. The total river length is given by the summation of river segments

of a certain Strahler order upstream from each station. The selected stations and stream orders are depicted in Fig. 1. The length of river segments ranges from 55 to 522 km, with a mean length of 190 km.

2.2 Methods

The methodology is primarily based upon the approach of Uhlemann et al. (2010). Here, we briefly describe the used methods and we focus mainly on the differences arising from the larger size of the study area.

2.2.1 Identification of flood peak discharges

The first step in this study is the selection of flood peaks at individual stations. The local maxima within the time series of mean daily discharges (Q_d) must be identified. Local maxima are Q_d values that are higher than values on both the previous and following days. If several consecutive days have exactly the same value of Q_d , the first day is used.

For each gauging station, most sets of local maxima are due to minor flow fluctuations. To select real flood peak discharges, the local maxima are compared with the 2-year return periods of mean daily discharges at a station (Q_2). Peak discharges that are equal to or greater than the 2-year return level are denoted as Q_p . Nevertheless, we assume that a serious flood must be characterized by even higher discharges at least in a part of the affected area. Therefore, we also search

for peak discharges that are equal to or greater than the 10-year return level of mean daily discharge (Q_{10}). The values of Q_2 and Q_{10} are estimated from the series of annual maxima of Q_d at a station. Each annual maxima series is approximated by the generalized extreme value distribution (GEV) using the maximum likelihood estimation method (Wilks, 2006).

2.2.2 Determination of flood events

A flood event is defined here as a group of time-related Q_p at various stations where at least one Q_p value equals or exceeds Q_{10} . However, Q_p values often do not occur exactly on the same day due to, e.g., the extent of the study area, the propagation of flood waves downstream, or the movement of the precipitation field. Therefore, a time window when Q_p values seem to belong to the same event is defined. After analyzing all of the data series, we chose a time window that includes 12 days before and 12 days after the occurrence of the first value of $Q_p \geq Q_{10}$. If there are other values of $Q_p \geq Q_{10}$ within that time span, the time window is further extended with respect to the date of this peak discharge. This time span is slightly longer than that used by Uhlemann et al. (2010), but this difference is reasonable because a larger area is studied here. Moreover, the values of Q_p systematically lag behind at hydrometric profiles on the Havel River and its largest tributary the Spree. This may be due to the lowland character of these basins permitting extensive spilling of water. However, the chosen time window may be too long in some cases because another atmospherically unrelated event may begin.

Therefore, we introduce an additional rule for dividing flood peaks that were identified as time-related but are in fact associated with different atmospheric causes. If more Q_{10} values are identified in some time series within an individual flood event and the time span between those peaks is at least 5 days long, we divide the peaks into two floods; otherwise, only one flood event is considered. Finally, only the highest Q_p in a time series is considered.

2.2.3 Extremity indices design

Over 150 flood events are identified in the period 1951–2013. Each event can be described by its extent expressed as a length of affected river network:

$$L = \sum_{i=1}^k l_i, \quad (1)$$

where l_i denotes the length of the river segment belonging to one of k stations where Q_2 is detected. The considered part of the river network upstream from station i consists of individual river segments of a certain order. Strahler's stream ordering method is used (Strahler, 1957) when the first order is assigned to a headstream. Stream orders increase when two

river segments of the same order meet. This method is dependent on the chosen layer of the river network. In this study, we use the European catchments and Rivers network system of the European Environment Agency (EEA, 2017). However, only rivers of certain orders are included in the river length l_i . If a station is located on a stream of the fourth order, we consider only this particular river segment upstream from the station. In the case of the fifth and sixth orders, also river segments of one lower order are counted. Two lower orders are considered when the station is located on the stream of the seventh and eighth orders.

Both the spatial extent of floods and the aspect of the discharge magnitudes must be incorporated into an extremity index for evaluating extreme flood events. To demonstrate the role of the threshold of the considered maximum discharges, we defined three index variants with differences in discharge limits and applied them to the identified flood events.

Generally, the index is derived from L by multiplying l_i by normalized peak discharges. The basic variant considers all of the Q_p values normalized by the respective exact value of the 2-year return period Q_2 :

$$E_2 = \sum_{i=1}^k \left(\frac{Q_{pi}}{Q_{2i}} l_i \right). \quad (2)$$

The modification of the extremity index involves changing the threshold of considered discharge values. Although all Q_p values are used in the basic variant calculation, two other variants labeled E_5 and E_{10} consider Q_p values that are equal to or greater than 5-year (Q_5) or 10-year return periods (Q_{10}). As in Eq. (2), the new Q_p values are normalized by the respective value of Q_5 or Q_{10} .

Finally, we select 30 major floods according to each of the three extremity index variants. As the total study period covers 63 years, we select approximately one flood per 2 years. This enables a comparison of the rankings of flood events with respect to the individual index variants. This comparison opens the discussion of the role of extremity index design.

The floods are sorted based on whether they occurred in the colder or warmer half of the year; the decisive day for classification is the mean point of the event. The mean day is found using the method of directional statistics, which was originally designed for the analysis of flood seasonality (Black and Werritty, 1997). However, it is applicable to the determination of the mean day of the flood event. The method transforms the day of Q_p occurrence into directional vectors in a circle representing 1 year and the mean vector is translated into the mean day of the event. The colder half-year is set from November to April; the events with a mean day between May and October are classified as warm half-year floods.

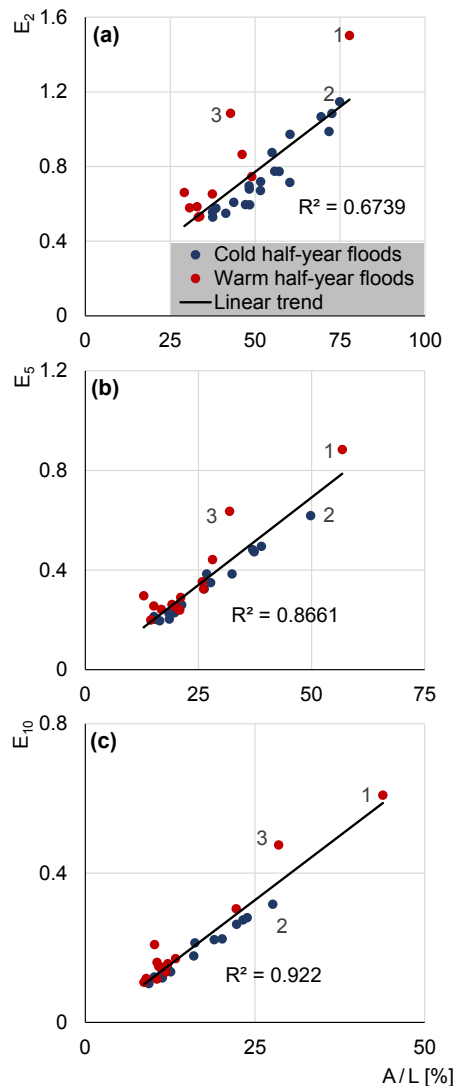


Figure 2. Relationship between the proportion of the affected river length (x axis) and the flood extremity E (y axis) according to E_2 (a), E_5 (b) and E_{10} (c). R^2 indicates the value of the coefficient of determination.

3 Results

The identified floods have various natures, from 1- or 2-day flood events caused mainly by localized convective precipitation to long-lasting and extensive cold half-year floods. Although the cold half-year events hit mostly larger areas than warm half-year floods, the flood of June 2013 was the largest one with respect to the affected river network. Flows higher than a 2-year return period occurred at about 13 700 km of the river network, which is 78 % of the total considered river length.

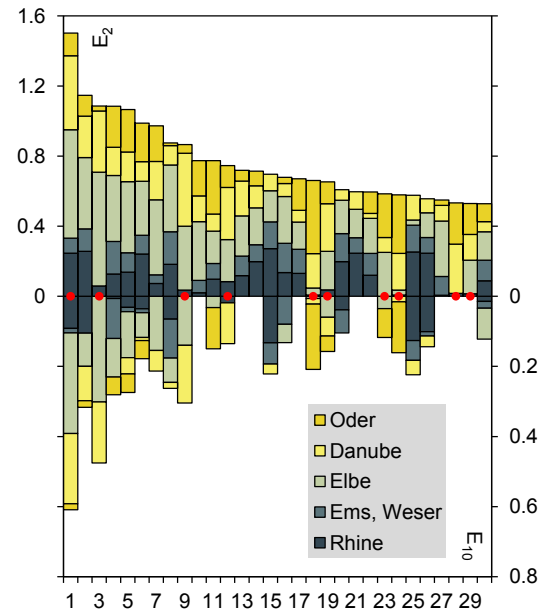


Figure 3. The 30 largest flood events in the study area from 1951 to 2013 according to E_2 and the corresponding events according to E_{10} . Missing bars indicate events which are not included in the set of 30 largest floods compiled by E_{10} . Contributions of individual river basins to the index value are distinguished by color. Red dots indicate warm half-year floods.

3.1 Comparison of the extremity index variants

As we mainly focus on extensive floods affecting more river basins at the same time, three lists of 30 major floods are created according to values of the index variants (Table 1). The events are listed with respect to the E_2 . Floods selected by E_2 are primarily extensive events as small flood discharges are also considered. The flood of June 2013 is the first of the major floods, followed by the March flood of 1988 and the flood of August 2002. Overall, there are 10 events in the warm half-year among 30 maxima. By contrast, the lists of floods according to the E_5 and E_{10} are more balanced from this point of view. They contain several events that are not present among the maxima according to E_2 ; most of these extra floods belong to the warm half-year. These floods replaced some cold half-year floods with relatively low values of Q_p . More floods with lesser extent are present in the lists according to the E_5 and E_{10} . Mainly the latter list contains relatively shorter and spatially limited May floods, which are associated with spring convection causing higher discharges. Nevertheless, three floods were evaluated as being at the maximum, regardless of the index variant, with only different ranking among them; the June flood of 2013 is the biggest according to each index variant.

Figure 2 depicts differences among the extremity index variants in terms of their dependence on the proportion of the affected river length A/L . Each chart in Fig. 2 represents

Table 1. List of 30 major floods according to the E_2 , E_5 and E_{10} indices. The date is displayed in the YYYY/MM/DD format. The A/L column refers to the proportion of the affected river length to the total length of the river network. Warm half-year floods are in bold.

Ranking	Flood duration	E_2	A/L (%)	E_5	Ranking	A/L (%)	E_{10}	Ranking	A/L (%)
1	2013/05/30–2013/06/17	1.50	78	0.88	1	57	0.61	1	44
2	1988/03/25–1988/04/08	1.15	75	0.62	3	50	0.32	3	28
3	2002/08/12–2002/08/23	1.09	43	0.64	2	32	0.48	2	28
4	1981/03/11–1981/03/30	1.08	73	0.48	5	37	0.28	5	24
5	2011/01/14–2011/01/29	1.07	69	0.50	4	39	0.27	6	23
6	1982/01/01–1982/01/17	0.99	72	0.38	9	32	0.18	12	16
7	2006/03/29–2006/04/12	0.97	60	0.38	8	27	0.21	10	16
8	2003/01/03–2003/01/19	0.88	55	0.47	6	37	0.26	7	22
9	1954/07/02–1954/07/21	0.87	46	0.44	7	28	0.30	4	22
10	1974/12/08–1974/12/26	0.77	56	0.20	28	16	–	–	–
11	1979/03/06–1979/03/30	0.77	57	0.21	26	15	0.15	18	12
12	1965/06/10–1965/06/20	0.75	49	0.32	13	26	0.14	22	12
13	1956/03/04–1956/03/14	0.72	52	0.23	24	20	–	–	–
14	1999/02/21–1999/03/07	0.71	60	–	–	–	–	–	–
15	1995/01/25–1995/02/12	0.70	48	0.35	11	28	0.22	9	19
16	1986/12/31–1987/01/10	0.68	48	0.26	18	21	0.13	23	11
17	1968/01/16–1968/01/28	0.67	52	–	–	–	–	–	–
18	1997/07/06–1997/07/24	0.66	29	0.30	14	13	0.21	11	10
19	1981/07/19–1981/07/30	0.65	37	0.35	10	26	0.16	15	12
20	1998/10/30–1998/11/13	0.61	44	0.24	22	20	0.10	30	9
21	1980/02/05–1980/02/18	0.60	47	0.20	27	19	–	–	–
22	2002/02/27–2002/03/12	0.59	48	–	–	–	–	–	–
23	1958/06/29–1958/07/16	0.58	33	0.29	15	21	0.12	27	9
24	1997/07/19–1997/08/02	0.58	31	0.26	19	15	0.16	14	11
25	1970/02/23–1970/02/28	0.58	38	0.32	12	26	0.22	8	20
26	1993/12/21–1993/12/30	0.56	37	0.26	16	21	0.14	19	12
27	1987/03/26–1987/04/11	0.55	41	–	–	–	–	–	–
28	1985/08/06–1985/08/28	0.53	34	0.25	20	20	–	–	–
29	1965/05/30–1965/06/10	0.53	33	–	–	–	–	–	–
30	1994/04/13–1994/04/27	0.53	37	0.23	25	18	0.12	25	10
34	2010/06/03–2010/06/14	–	–	0.24	23	21	–	–	–
35	2011/01/04–2011/01/14	–	–	0.20	30	16	0.12	24	11
39	1977/08/24–1977/09/13	–	–	0.20	29	14	–	–	–
40	1977/08/01–1977/08/16	–	–	–	–	–	0.11	29	9
44	2005/08/22–2005/08/26	–	–	0.24	21	17	0.15	17	11
47	1999/05/20–1999/05/27	–	–	0.26	17	19	0.17	13	13
60	2010/05/18–2010/06/01	–	–	–	–	–	0.15	16	11
65	1999/05/13–1999/05/19	–	–	–	–	–	0.14	20	12
66	1955/01/14–1955/01/21	–	–	–	–	–	0.14	21	13
72	1983/04/10–1983/04/21	–	–	–	–	–	0.12	26	11
87	1983/05/25–1983/05/31	–	–	–	–	–	0.12	28	11

one variant of the extremity index. The correlation between A/L and the index values is much higher when the discharge threshold is set to a 10-year return period. If we only consider such high discharges, the summation of the affected river length will approach the index values. The correlation is not so close in the case of Fig. 2a. The placement of cold and warm half-year events has a specific character in Fig. 2. The cold half-year floods are more extensive and have lower index values compared to the floods of the warm half-year, which applies to each chart. The rankings of the three high-

lighted flood events remain close, regardless of the variant. However, relatively smaller discharges of the March 1988 flood cause the decrease in its E_5 and E_{10} values. By contrast, the extremity of the June 2013 flood is even more highlighted in Fig. 2c as it significantly departs from other events. This is also shown in Fig. 3 representing the differences between E_2 and E_{10} values for 30 individual events. In the case of E_{10} both the June 2013 and August 2002 floods reach much higher index values than the rest of the events. Floods are ranked as in Table 1.

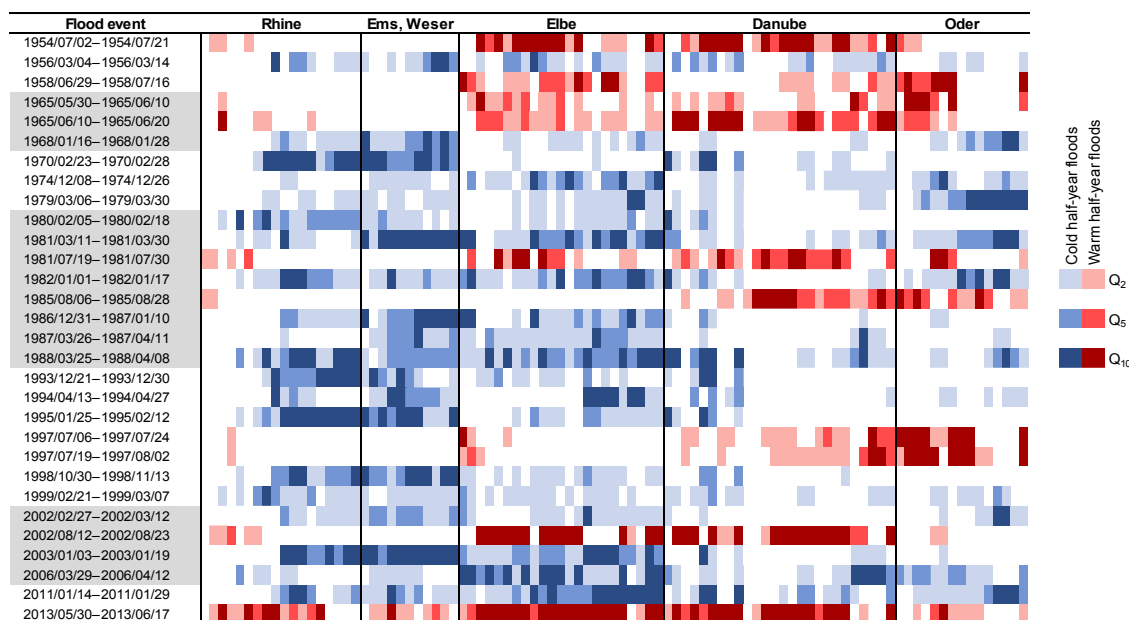


Figure 4. The occurrence of discharges equal to or greater than 2-, 5- and 10-year flood at individual stations during each of the 30 maximum floods according to the E_2 index. The basins are indicated at the top of the chart; the stations are arranged according to their position downstream.

3.2 Major flood characteristics

Figure 3 indicates large spatial differences among the flood events. It is clear that the warm half-year floods relate more to the Oder, Danube and Elbe River basins. The Rhine River basin is less represented and, in the Weser and Ems River basins, the warm half-year floods rarely occur. A more comprehensive insight into this issue is provided in Fig. 4. The occurrence of flood discharges in the basins is demonstrated on 30 maximum floods according to E_2 . The differences are evident within the individual basins. There is a shift from warm to cold half-year floods when we move from the upper Rhine or Oder downstream. The Warta, a main tributary of the Oder, is affected mainly by cold half-year events. However, the last displayed station is located on the Oder River. Within the Danube basin, a gap in the occurrence of cold half-year floods is visible in the middle part of the basin. Some consecutive flood events are similar to each other, which is due to the fact that they both occur in a relatively short time. The first event has an effect on the initiation of the second one, which is the case for a pair of floods in June 1965 and July 1997. The flood of June 2013 is unique as it is the only event which largely affected the Weser and Rhine basins.

3.2.1 Seasonal distribution

Floods of the cold half-year are generally better represented among the major flood events. The seasonal distribution is quite similar for E_2 and E_{10} , with a frequency maximum in

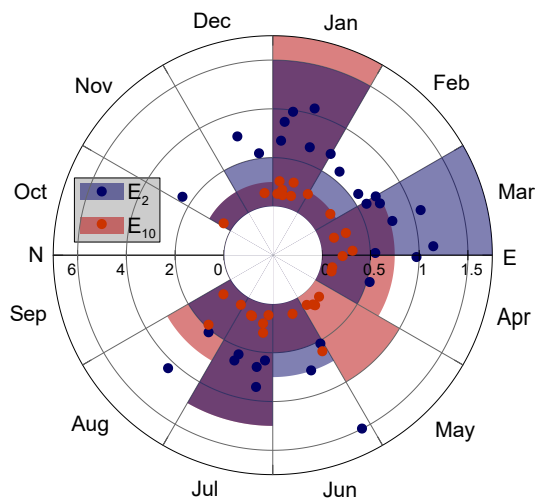


Figure 5. Seasonal distribution of 30 maximum floods according to E_2 and E_{10} indices. The number of extreme floods in individual months N is depicted by shading; the mixed color indicates overlapping data. The signs represent mean calendar days of the events; the distance of the sign from the center of the diagram reflects the flood extremity given by the values of E_2 and E_{10} .

winter and a secondary maximum in summer (Fig. 5). According to E_2 , major events are concentrated in January and March, but the March floods are not so pronounced in the case of E_{10} . The secondary frequency maximum occurs in July and for both indices has a similar character. Surprisingly, a great difference arose in the number of extreme floods in

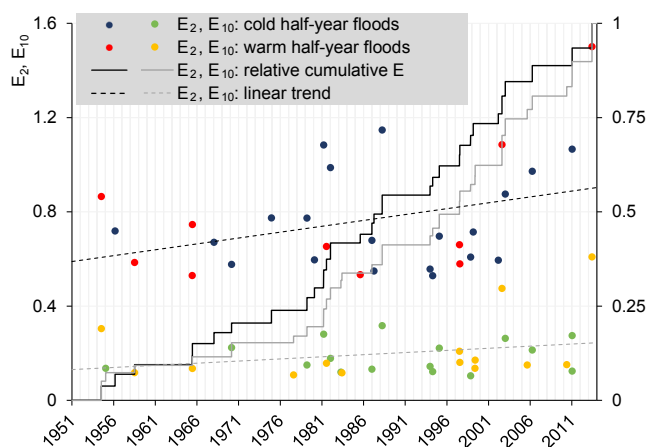


Figure 6. Interannual variability of 30 major floods according to E_2 and E_{10} . The symbols represent the extremity of cold and warm half-year floods with respect to E_2 and E_{10} ; lines depict linear trends and relative cumulative values of the flood extremity.

May. These are spatially limited events, which moved up in ranking due to higher discharges. The rest of the year is characterized by a low frequency of major floods. Only a single major flood occurred from late August to the beginning of December. It began at the end of October 1998, but the mean day of the event lies in November. Its extremeness was surprisingly high, mainly according to the E_2 variant of the extremity index.

3.2.2 Interannual variability

Major floods do not occur regularly over time. Some clusters of flood events are apparent in Fig. 6, which presents the distribution of major floods between 1951 and 2013. The July flood of 1954 is the first recorded flood in the period examined. A significant accumulation of flooding is apparent in the 1980s and from 1993 to 2006. By contrast, a long period without major floods occurred at the beginning of the 1960s. The first 15 years have only one flood of the cold half-year.

Generally, there are more major floods in the second half of the period, which applies to both index variants. It seems that the number of events increases mainly from the 1980s, as is their extremity. However, the extremity according to E_2 increases more rapidly.

3.2.3 Spatial distribution

Regarding the spatial distribution of floods, Fig. 3 demonstrates that floods during the warm half-year relate more to the Oder, Danube and Elbe River basins. Warm half-year floods are less frequent in the Rhine River basin, and they occur very rarely in the Weser and Ems River basins, where cold half-year floods dominate. This is confirmed by Fig. 7, which depicts the frequency of 30 major floods in both half-years within individual gauge stations.

In general, the number of cold half-year floods decreases towards the southeast, whereas the number of warm half-year floods increases in the same direction. Regardless of the variant of the extremity index, there are regions affected by extreme floods only in one part of the year. This is true for the Weser, Ems, and the lower part of the Rhine River basin including the Main (cold half-year) and most of the Alpine rivers (warm half-year). By contrast, other regions are prone to extreme floods in both the cold and warm halves of the year: the Oder, Elbe and Danube River basins, apart from the Alpine tributaries. However, a low number of identified floods does not exclude their occurrence at individual stations. It means that floods in a given location are not part of large-scale cold or warm half-year floods, which were evaluated in this study.

4 Discussion and conclusions

This paper addresses the evaluation of major flood events in the transitional area between western and central Europe in the period 1951–2013. Major floods are defined according to the value of a flood extremity index. We created three variants of the index with differences in terms of discharge thresholds. We were motivated by Uhlemann et al. (2010) and Schröter et al. (2015), who used similar flood extremity indices, with only a difference in the threshold of the discharge values entered into the calculation. Uhlemann et al. (2010) used a 2-year flow threshold, while Schröter et al. (2015) chose a higher limit of a 5-year flow, thus making these studies incomparable. In this paper, we introduce the differences that arise in the resulting lists of major floods when we use indices with different discharge thresholds. We selected the value of Q_2 as a basic threshold and two additional threshold values: Q_5 and Q_{10} . We found that the value of this threshold is crucial for the ranking of major floods. The number of warm half-year floods slightly increases in the lists of major floods when using the higher discharge thresholds. Two sets of 30 major floods are presented according to E_2 and E_{10} indices, and the respective lists are compared in terms of seasonality, interannual variability and spatial distribution.

Generally, the lists of major floods are quite similar to the list of German trans-basin floods presented by Uhlemann et al. (2010) because Germany covers more than half of the area studied in this work. The duration of “identical” floods is slightly different, as is their ranking. This is mainly due to the different size of the area of interest. Schröter et al. (2015) used an index similar to Uhlemann et al. (2010), but the authors only offered a comparison of the extremity of three summer flood events: the floods of 1954, 2002 and 2013. The flood event of 2013 is reported as the largest, followed by the flood of 1954. In this paper, the flood of August 2002 is always more extreme than the flood of 1954, regardless of the index variant used, because of the differences in the extent

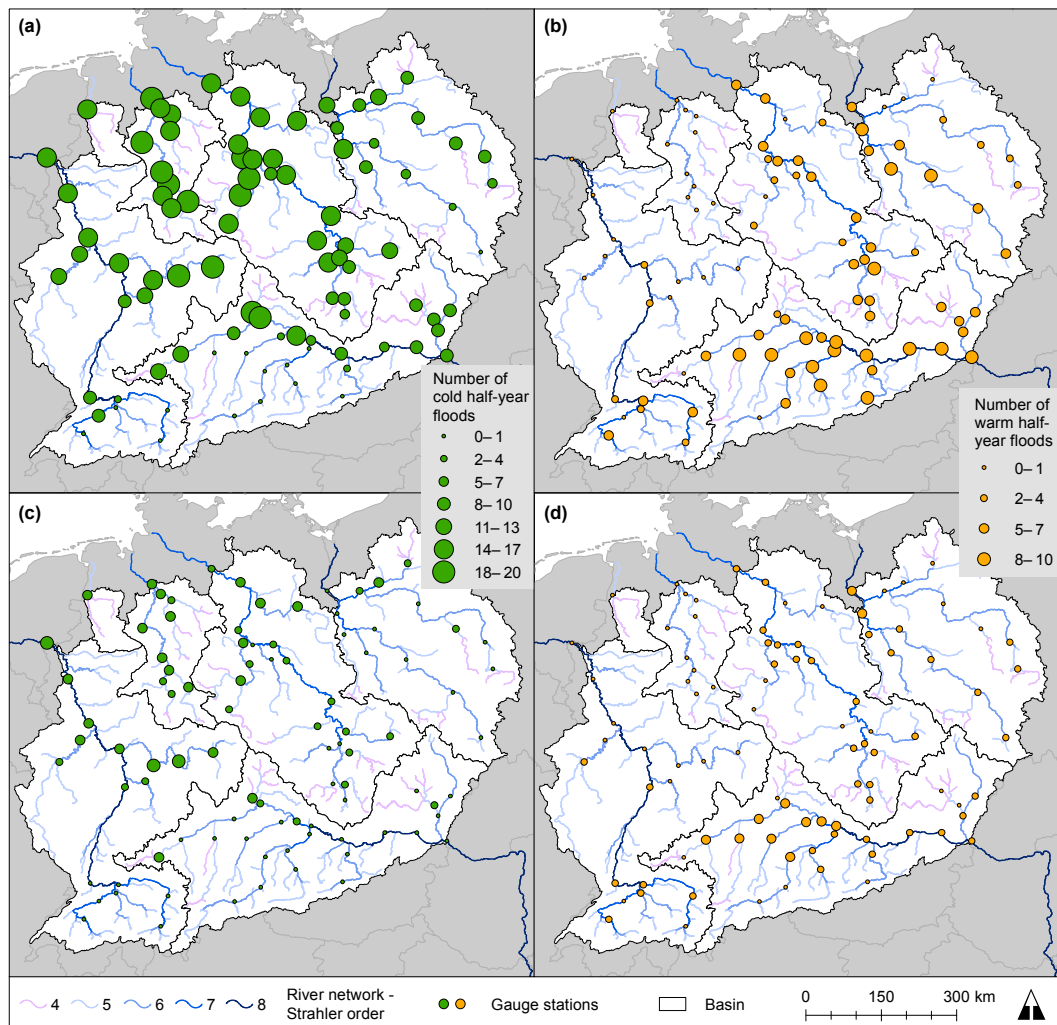


Figure 7. Spatial distribution of 30 maximum floods according to E_2 (a, b) and E_{10} (c, d). The numbers of cold (a, c) and warm (b, d) half-year floods identified in individual gauge stations during 1951–2013 are depicted by circle size.

of the area of interest. Nevertheless, the flood of June 2013 remains on top of the lists.

We can also compare our results with those of Barredo (2007), who provided a set of 21 large European river floods compiled according to the amount of damage caused. Six of these floods affected our area of interest; all are included in the set of major floods according to E_{10} , but only four belong to the 30 major events with respect to E_2 . Obviously, floods that caused major damage are better represented by the variant of the extremity index, with a higher threshold of considered discharge values. From this point of view, the E_{10} index might be better able to identify major floods, which however noticeably depart from other events.

Regarding the seasonal distribution of major flood events, the predominance of cold half-year floods is apparent in both lists. Uhlemann et al. (2010) showed the same result. By contrast, floods during the warm half of the year dominate the list of the 30 major floods in the Czech Republic by Müller

et al. (2015). This may be due to the fact that the occurrence of warm half-year floods is increasing from the northwest to the southeast in the studied area.

The temporal distribution of major flood events during the period between 1951 and 2013 is rather uneven. There are certain clusters in terms of the occurrence of major floods. Some periods of reduced or increased frequencies of major flooding are identical to the results of other papers (Uhlemann et al., 2010; Müller et al., 2015). For example, we found these identical trends: a higher frequency of major floods in the 1980s and a decline in the number of identified floods in the 1990s. The 5-year period between 2006 and 2010 is different, however, because it is a period with a higher frequency of major flooding in Müller et al. (2015). The increase in major flooding in the second half of the period is again consistent with the findings of Uhlemann et al. (2010). However, it remains unclear whether this is a trend or just a part of a cycle. In recent years, there has been a discussion

about increasing flood risk due to ongoing climate change and anthropogenic modifications of the landscape and especially floodplains. On a local level, the runoff is influenced by the changes in land use, riverbeds or the surface drainage, which often lead to runoff acceleration and steeper flood waves (Langhammer and Vilímek, 2008). By contrast, the construction of water reservoirs can reduce a flood. The Slapy Dam at the Vltava River was only partially filled before the flood of July 1954. Unaffected discharge of $2920 \text{ m}^3 \text{ s}^{-1}$ would be the second largest in Prague in the 20th century after the flood of March 1940; the actual discharge was only $2240 \text{ m}^3 \text{ s}^{-1}$ (Brázdil et al., 2005). However, the effect of local landscape changes can be less significant for extensive events, as it depends on the flood extremity (Langhammer and Vilímek, 2008).

The temporal characteristics of major flood events are also connected with the opposite extreme. The historical records show that an extreme flood was followed by a great drought in some cases (Brázdil et al., 2005). Lloyd-Hughes and Saunders (2002) conclude that the greater pan-European droughts occurred in the early 1950s and the 1990s; lesser drought incidence is apparent in the 1980s. For the analysis, they used the Palmer drought severity index and standardized precipitation indices calculated at different timescales.

At a shorter timescale, the wetness conditions are crucial for flood initiation; antecedent soil moisture can highly influence the flood extremity. The June 2013 flood was the case when great precipitation amounts coincided with high antecedent soil moisture and produced an exceptional flood (Blöschl et al., 2013). The effect of antecedent wetness conditions depends on the season and a type or an extremity of flood. High antecedent soil moisture relates in particular to cold half-year floods, while the signal varies in warm half-year cases (Nied et al., 2013).

Further research on the topic of extreme floods will examine the related meteorological conditions. A comprehensive evaluation of antecedent wetness conditions, causal atmospheric circulation, the consequent precipitation and the flow response is needed. A comparison of major floods with precipitation and circulation extremes would be useful for a better understanding of the causes of extensive floods, which affect several river basins.

Data availability. Mean daily discharge data were mainly provided by the Global Runoff Data Centre (GRDC, 2017). Some data are accessible via the Austrian server eHYD (2016) at <http://ehyd.gv.at/> and the Polish Institute of Meteorology and Water Management – National Research Institute (IMGW-PIB, 2017) at <https://dane.imgw.pl/>. Data of the Czech Hydrometeorological Institute were purchased for research purposes. The European catchment and river network system (EEA, 2017) was used to determine the lengths of affected river networks.

Competing interests. The authors declare that they have no conflict of interest.

Acknowledgements. This work was supported by the Czech Science Foundation (grant number 17-23773S). Acknowledgements also belong to the Global Runoff Data Centre and the Czech Hydrometeorological Institute for providing runoff data.

Edited by: Vazken Andréassian

Reviewed by: two anonymous referees

References

- Barredo, J. I.: Major flood disasters in Europe: 1950–2005, *Nat. Hazards*, 42, 125–148, <https://doi.org/10.1007/s11069-006-9065-2>, 2007.
- Bebber van, W. J.: Die Zugstrassen der barometrischen Minima nach den Bahnenkarten der Deutschen Seewarte für den Zeitraum 1875–1890, *Meteorol. Z.*, 8, 361–366, 1891.
- Beniston, M., Stephenson, D. B., Christensen, O. B., Ferro, C. A. T., Frei, C., Goyette, S., Halsnaes, K., Holt, T., Jylhä, K., Koffi, B., Palutikof, J., Schöll, R., Semmler, T., and Woth, K.: Future extreme events in European climate: an exploration of regional climate model projections, *Climatic Change*, 81, 71–95, <https://doi.org/10.1007/s10584-006-9226-z>, 2007.
- Black, A. R. and Werritty, A.: Seasonality of flooding: a case study of North Britain, *J. Hydrol.*, 195, 1–25, 1997.
- Blöschl, G., Nester, T., Komma, J., Parajka, J., and Perdigão, R. A. P.: The June 2013 flood in the Upper Danube Basin, and comparisons with the 2002, 1954 and 1899 floods, *Hydrol. Earth Syst. Sci.*, 17, 5197–5212, <https://doi.org/10.5194/hess-17-5197-2013>, 2013.
- Brázdil, R., Glaser, R., Pfister, C., Dobrovolný, P., Antoine, J.-M., Barriandos, M., Camuffo, D., Deutsch, M., Enzi, S., Guidoboni, E., Kotyza, O., and Rodrigo, F. S.: Floods events of selected European rivers in the sixteenth century, *Climatic Change*, 43, 239–285, 1999.
- Brázdil, R., Dobrovolný, P., Elleder, L., Kakos, V., Kotyza, O., Květoň, V., Macková, J., Müller, M., Štekl, J., Tolasz, R., and Valášek, H.: Historical and Recent Floods in the Czech Republic, Masaryk University and Czech Hydrometeorological Institute, Brno, Prague, Czech Republic, 2005.
- Caspary, H. J.: Recent winter floods in Germany caused by changes in the atmospheric circulation across Europe, *Phys. Chem. Earth*, 20, 459–462, 1995.
- EEA: European catchments and Rivers network system, <https://www.eea.europa.eu/data-and-maps/data/european-catchments-and-rivers-network>, last access: 13 March 2017.
- eHYD: Hydrographic data of Austria, <http://ehyd.gv.at/>, last access: 9 May 2016.
- Francou, J. and Rodier, J.-A.: Essai de classification des crues maximales observées dans le monde, *Cah. Orstom Hydrol.*, IV, 19–46, 1967.
- GRDC: River discharge data, <http://www.bafg.de/GRDC/>, last access: 23 February 2017.

- Herschey, R. W. (Ed.): World Catalogue of Maximum Observed Floods, IAHS Press, Wallingford, IAHS-AISH Publ. 284, 2003.
- IMGW-PIB: Central database, <https://dane.imgw.pl/>, last access: 26 February 2017.
- Jacobeit, J., Glaser, R., Luterbacher, J., and Wanner, H.: Links between flood events in central Europe since AD 1500 and large-scale atmospheric circulation modes, *Geophys. Res. Lett.*, 30, 1172–1175, <https://doi.org/10.1029/2002GL016433>, 2003.
- Keef, C., Svensson, C., and Tawn, J. A.: Spatial dependence in extreme river flows and precipitation for Great Britain, *J. Hydrol.*, 378, 240–252, 2009.
- Kundzewicz, Z. W., Ulbrich, U., Brucher, T., Graczyk, D., Kruger, A., Leckebusch, G. C., Menzel, L., Pinskiwar, I., Radziejewski, M., and Szwed, M.: Summer floods in Central Europe – climate change track?, *Nat. Hazards*, 36, 165–189, 2005.
- Langhammer, J. and Vilímek, V.: Landscape changes as a factor affecting the course and consequences of extreme floods in the Otava river basin, Czech Republic, *Environ. Monit. Assess.*, 144, 53–66, <https://doi.org/10.1007/s10661-007-9941-6>, 2008.
- Lloyd-Hughes, B. and Saunders, M. A.: A drought climatology for Europe, *Int. J. Climatol.*, 22, 1571–1592, <https://doi.org/10.1002/joc.846>, 2002.
- Mudelsee, M., Börngen, M., Tetzlaff, G., and Grünwald, U.: No upward trends in the occurrence of extreme floods in central Europe, *Nature*, 425, 166–169, 2003.
- Müller, M. and Kašpar, M.: Quantitative aspect in circulation type classifications – an example based on evaluation of moisture flux anomalies, *Phys. Chem. Earth*, 35, 484–490, <https://doi.org/10.1016/j.pce.2009.09.004>, 2010.
- Müller, M. and Kaspar, M.: Event-adjusted evaluation of weather and climate extremes, *Nat. Hazards Earth Syst. Sci.*, 14, 473–483, <https://doi.org/10.5194/nhess-14-473-2014>, 2014.
- Müller, M., Kašpar, M., Valeriánová, A., Chřová, L., Holtanová, E., and Gvoždíková, B.: Novel indices for the comparison of precipitation extremes and floods: an example from the Czech territory, *Hydrol. Earth Syst. Sci.*, 19, 4641–4652, <https://doi.org/10.5194/hess-19-4641-2015>, 2015.
- Munich Re: Topics Geo Natural Catastrophes 2014: Analyses, Assessments, Positions, Munich Reinsurance Company, Munich, Germany, 2015.
- Nied, M., Hündecha, Y., and Merz, B.: Flood-initiating catchment conditions: a spatio-temporal analysis of large-scale soil moisture patterns in the Elbe River basin, *Hydrol. Earth Syst. Sci.*, 17, 1401–1414, <https://doi.org/10.5194/hess-17-1401-2013>, 2013.
- Nissen, K. M., Ulbrich, U., and Leckebusch, G.: Vb cyclones and associated rainfall extremes over Central Europe under present day and climate change conditions, *Meteorol. Z.*, 22, 649–660, <https://doi.org/10.1127/0941-2948/2013/0514>, 2014.
- Rodda, H. J. E.: The Development and application of a flood risk model for the Czech Republic, *Nat. Hazards*, 36, 207–220, 2005.
- Rodier, J. A. and Roche, M. (Eds.): World Catalogue of Maximum Observed Floods, IAHS Press, Wallingford, IAHS Publ. 143, 1984.
- Schröter, K., Kunz, M., Elmer, F., Mühr, B., and Merz, B.: What made the June 2013 flood in Germany an exceptional event? A hydro-meteorological evaluation, *Hydrol. Earth Syst. Sci.*, 19, 309–327, <https://doi.org/10.5194/hess-19-309-2015>, 2015.
- Strahler, A. N.: Quantitative analysis of watershed geomorphology, *EOS T. Am. Geophys. Un.*, 38, 913–920, 1957.
- Uhlemann, S., Thielen, A. H., and Merz, B.: A consistent set of trans-basin floods in Germany between 1952–2002, *Hydrol. Earth Syst. Sci.*, 14, 1277–1295, <https://doi.org/10.5194/hess-14-1277-2010>, 2010.
- Wilks, D. S.: Statistical Methods in the Atmospheric Sciences, 2nd Edn., Academic Press, Burlington, USA, 2006.